

## Evaluation of EC stray radiation in ITER and its implication for diagnostics

---

**Antoine Sirinelli<sup>\*a</sup>, Franco Gandini, Mark Henderson, Johan W. Oosterbeek<sup>b</sup> and George Vayakis**

*ITER Organization*

*Route de Vinon-sur-Verdon, CS 90 046, 13067 St. Paul Lez Durance Cedex, France.*

<sup>a</sup>*Fircroft Engineering*

*Lingley House, 120 Birchwood Point, Birchwood Boulevard, Warrington, WA3 7QH, UK.*

<sup>b</sup>*Eindhoven University of Technology*

*P.O. Box 513, 5600 AZ, Eindhoven, The Netherlands.*

*E-mail: [Antoine.Sirinelli@iter.org](mailto:Antoine.Sirinelli@iter.org)*

During normal ITER operation, Electron Cyclotron (EC) heating and current-drive system will generate stray microwave radiations. Three cases have been identified with their associated load localisation and power. The effect on first-wall diagnostics, mineral insulated cables and vacuum windows are described. The most affected diagnostic port plugs are the #11, #12 and #17. In these areas, mitigation strategies will have to be found to protect the vacuum windows from the cross-polarised stray radiation.

*1st EPS conference on Plasma Diagnostics*

*14-17 April 2015*

*Frascati, Italy*

---

<sup>\*</sup>Speaker.

## 1. Introduction

ITER will use an Electron Cyclotron (EC) system for heating, current drive (CD) and breakdown assistance [1]. Up to 20 MW of microwave power at 170 GHz will be coupled to the plasma. The beams will be launched from 4 upper ports and 1 equatorial port. In the equatorial port #14, 3 launchers are available: the top launcher is emitting counter ECCD with a toroidal angle of  $20^\circ$ ; middle and bottom launchers are emitting co-ECCD with a toroidal angle of  $25^\circ$ . The localisation of EC equatorial port in ITER vacuum vessel is shown on Figure 1.

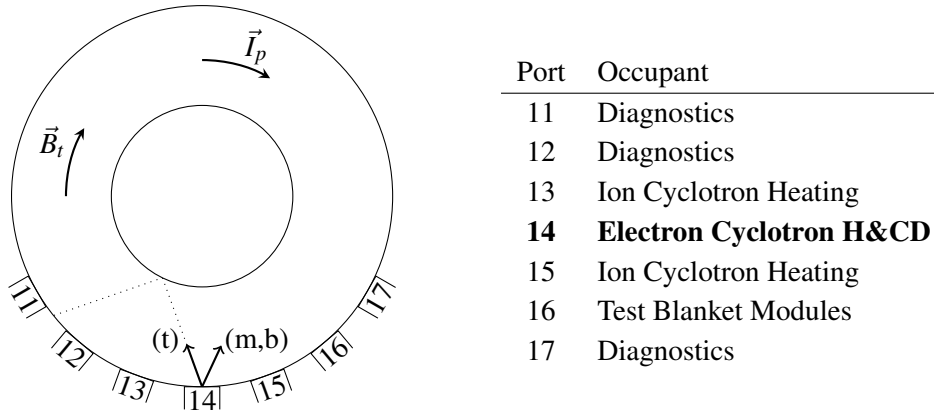


**Figure 1:** Implementation of ITER equatorial ports around EC equatorial launchers, viewed from the top of the tokamak. EC toroidal launching directions are indicated for the top (t), middle (m) and bottom (b) launchers. Neighbouring ports are identified by their numbers and the occupants are listed in the table. For the direct beam case, the approximated beam path is shown with a dotted line.

In normal operation, for heating and current drive, most of the injected power is absorbed by the plasma but a fraction will be able to reach the first wall (FW) or diagnostic systems. This stray radiation can increase the heat loads these components are exposed to.

The different cases are described in section 2 with their associated stray radiation levels and locations. The effects on the diagnostics are described in section 3.

## 2. Stray radiation conditions

Three conditions have been identified as sources of EC stray radiation: direct beam, cross-polarised beam and background power.

### 2.1 Direct beam

For breakdown assistance, EC system will be used, for a limited time, to produce free electrons helping the initial avalanche. The EC beams will launch up to 6 MW for up to 5.5 s from either the equatorial or one upper launcher towards the High Field Side (HFS). During the first phase of ITER, when blanket modules are not present, a dedicated deflector on the HFS is installed to protect the vacuum vessel and the in-vessel component from the incident beam. During the second phase of ITER, the beam will be directed to the blankets, avoiding gaps and gripping features. The blanket or the deflector are reflecting the beam toward the Low Field Side (LFS). There, the beam will interact with in-vessel components.

Launcher	Elevation (Z)	Poloidal angle ( $\alpha$ )	Toroidal angle ( $\beta$ )
top	1.27 m	$-12^\circ$ to $12^\circ$	$-22^\circ$ to $-18^\circ$
middle	0.62 m	$0^\circ$ to $32^\circ$	$23^\circ$ to $27^\circ$
bottom	$-0.03$ m	$-32^\circ$ to $-10^\circ$	$23^\circ$ to $27^\circ$

**Table 1:** Simulated steering angles for the 3 equatorial EC launchers.

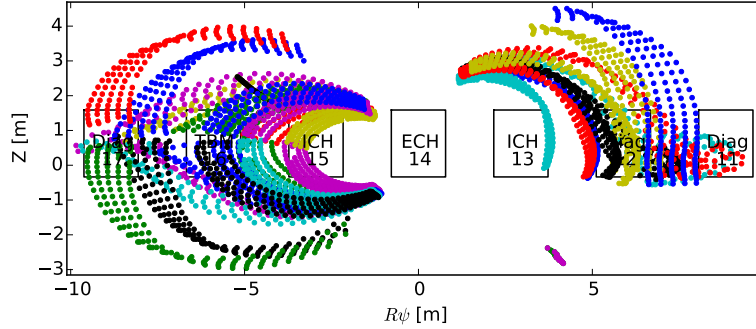


**Figure 2:** Localisation of the EC beam spots on the ITER First Wall after X-mode refraction. The LFS side of the tokamak is unwrap and the port are displayed. Each colour corresponds to a scenario simulated.

Geometrical assessment has indicated that this beam will illuminate an area located around the diagnostic equatorial ports #11 (for the equatorial launcher, see Figure 1) or #17 (for the upper launcher). The peak EC power density has also been evaluated, from the Gaussian beam divergence, to be  $3 \text{ MW m}^{-2}$  on the LFS First Wall.

## 2.2 Cross-polarised beam

In normal operation, the EC wave is linearly polarised with its electric field nominally parallel to the plasma magnetic field (Ordinary mode or O-mode). A small fraction (minimised through calibration and/or active systems) is launched in the orthogonal polarisation, with electric field perpendicular to the magnetic field (Extraordinary mode or X-mode). This beam is reflected without any absorption and illuminates the first wall with a relatively small spot.

In order to estimate the localisation of the incident beam on the FW, TORBEAM [2] beam tracing code has been used. The plasma temperature foreseen in ITER (above 20 keV) is not compatible with the common cold plasma approximation used usually for wave propagation [3], therefore TORBEAM has been ran taking into account relativistic effects.

A set of equilibria has been chosen to reflect the diversity of plasma scenario: 15 MA DT plasma ( $Q=10$ ), 9 MA DT plasma ( $Q=5$ ), 12.5 MA hybrid scenario and 10 MA H-mode ramp-up phase. Furthermore, density and temperature profiles have been scanned in order to take into account the expected deviation from ideal plasma operation. Finally all the possible beam angle and launchers have been tried for the equatorial EC launcher. They are summarised in Table 1.

The results of the simulations are shown on Figure 2. A large portion of the LFS first wall will potentially receive this cross-polarised refracted beam. Blanket gaps are affected but also Ion Cyclotron Heating (ICH) ports, a Test Blanket Module (TBM) port and 3 diagnostic ports (#11, #12, #17).

The affected diagnostic ports host various diagnostics: visible and IR imaging, spectroscopy or microwave diagnostics. They all have aperture on the diagnostic FW followed by mirrors, waveguides, detectors or vacuum windows. This means that through the FW apertures, EC stray radiation will be able to reach some of these critical elements.

The evaluation of power arriving on the FW is done by simple geometrical assumptions from the length of the path and the Gaussian beam divergence, assuming 5 % of the power is transmitted in X-mode. More detailed analysis are not yet possible as the Gaussian optics in the EC equatorial launcher are being redesigned at the moment. It has been evaluated that the peak power expected on the LFS FW is about  $1.25 \text{ MW m}^{-2}$ . The cross-polarisation event can not be easily tracked during operation, leading to the assumption that this level of load can last during all EC operation.

### 2.3 Background power

Non-absorbed EC waves, as described in the previous cases but also in normal operation, will have multiple reflections on the metallic components of the vacuum vessel leading to a lower intensity and more homogeneous background stray radiation. A power balance approach [4, 5] has been taken, leading to a maximum of  $0.12 \text{ MW m}^{-2}$  load on FW aperture during startup (5.5 s maximum) and  $20 \text{ kW m}^{-2}$  during normal operation.

## 3. Effects of EC stray radiation on diagnostic components

The worst case scenario identified in Section 2 is the cross-polarisation case when  $1.25 \text{ MW m}^{-2}$  can be directed to the LFS first wall for a up to 3600 s. Different diagnostic parts have been identified receiving directly this incident power: diagnostic FW, FW samples, mirrors, Mineral Insulated (MI) cables, vacuum windows and silicon detectors.

### 3.1 Diagnostic first wall, first wall samples and mirrors

Different diagnostic components are facing the plasma and thus directly exposed to EC stray radiations. Diagnostic ports are protected by a stainless steel FW [6]; diagnostic FW samples [7] are installed in the blankets; mirrors are placed in front of FW aperture to direct light toward recessed sensors. These plasma facing components are made of stainless steel, beryllium or molybdenum. All of them are good conductors which will reflect most of the incoming EC wave. Nevertheless, a small fraction will be absorbed by ohmic heating on the metal surface. The absorbed fraction can be calculated for a perfect material surface:  $A = \sqrt{16\pi f \epsilon_0 / \sigma}$  where  $f$  is the incident wave frequency,  $\epsilon_0$  the vacuum permittivity and  $\sigma$  the metal conductivity. Furthermore, it has been observed that surface roughness plays a role and can increase the absorbed power by a factor of 2. The maximum absorbed power on surface for all the exposed component materials is shown in Table 2.

These components are designed to handled direct plasma radiation up to  $350 \text{ kW m}^{-2}$  and nuclear heating. They are therefore actively cooled. The additional load due to EC stray radiation is low compared to the other loads. For these FW diagnostic components, EC stray radiation is not foreseen to be an issue.

Material	Absorbed fraction	Absorbed power
Cu	0.2 %	2.5 kW m <sup>-2</sup>
Mo	0.4 %	5 kW m <sup>-2</sup>
Be	0.8 %	10 kW m <sup>-2</sup>
St. Steel 316LN	1.7 %	21 kW m <sup>-2</sup>

**Table 2:** Surface absorption of cross-polarised EC stray radiation for typical metals on ITER FW. Absorbed power given for an incident EC wave of 1.25 MW m<sup>-2</sup>.

Fused silica window parameters	
$\varnothing$	110 mm
$h$	12.5 mm
density	2.2 g cm <sup>-3</sup>
$\epsilon'_r$	3.8
$\tan \delta$	$3 \times 10^{-4}$
$C_p$	800 J kg <sup>-1</sup> K <sup>-1</sup>

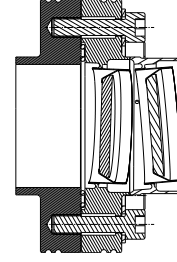


**Figure 3:** Fused silica window assembly used for equatorial port #11 reflectometry system and its associated parameters[8].

### 3.2 Mineral insulated cables

Magnetic flux loops and microfission chamber diagnostics will use MI cables of diameter in the range of 1 mm to 6 mm. While they are mostly running behind blanket modules, they might be locally exposed to EC stray radiation through the blanket gaps. The blanket structure being made of beryllium and stainless steel, the EC power will not loose so much power rattling in the gap before reaching the MI cable. MI cables are made of a stainless steel outer shell of at least 100  $\mu$ m which is much thicker than the EC skin depth  $\delta = (\mu \sigma \pi f)^{-1/2} \approx 1 \mu$ m where  $\mu$  is the permeability of the metal. EC stray radiation is not penetrating the MI cable and the loads are only on the surface of the cable according to Table 2.

Analysis have been carried out and shown locally a large increase of temperature of the MI cable under EC stray radiation exposure. Cable temperature can raise from 150 °C without EC stray radiation up to 480 °C. While this maximum temperature is below the maximum operating temperature, temperature induced electromotive force will produce noise on the flux loop measurement.

### 3.3 Vacuum windows

Most diagnostic systems will have their detectors outside of the vacuum vessel and even in the diagnostic building. Microwave, laser and Visible/IR systems will rely on vacuum windows to guide their beam outside the vessel. Vacuum windows will be double with monitored inter-space as safety measure for tritium confinement as shown in Figure 3. While the windows are recessed far from the FW, in some cases the EC stray radiation at FW level will go through an aperture and propagate through mirrors or waveguides up to the window. In this case the EC stray power level going through the window is defined by the FW aperture.

Most windows will be made of fused silica, a good microwave transmitter but nevertheless a lossy material. Part of the EC stray radiation will be absorbed by the windows. The absorbed power

can be written as  $P_{abs} = (1 - e^{-2\alpha h})P_{in}$  with  $P_{in}$  the incident EC power,  $h$  the window thickness and  $\alpha$  the attenuation factor.  $\alpha = \pi f \sqrt{\epsilon_r'} \tan \delta / c$  with  $\epsilon_r'$  the relative permittivity of the dielectric,  $\tan \delta$  its loss tangent and  $c$  the speed of light.

For the reflectometry system in equatorial port #11, the FW aperture is a corrugated circular waveguide of 63.5 mm diameter. In the cross polarised stray radiation case, the power arriving at the windows is then  $P_{in} \approx 4\text{kW}$  and the absorbed power by each disc is  $P_{abs} \approx 100\text{W}$ .

The window discs are maintained on the assembly by a small ferrule which does not allow so much heat dissipation. A simple approach, neglecting the heat flow through the ferrule will see an increase of the window temperature of about 30 K per minute. While the windows will be able to sustain the EC stray radiation for a couple of minutes, it is likely that a mechanism will have to be designed to prevent damaging them if the stray radiation level cannot be reduced. A passive protection could be, for windows used for visible or IR measurement, to coat them with a microwave reflective layer. For the microwave diagnostics, in-waveguide notch filters are also an option. An active protection would require a set of sensing devices distributed in the vacuum vessel and ports. They could force EC system to change the launcher used or to activate shutters to be implemented in front of the windows exposed to high EC stray radiation.

#### 4. Conclusions

EC stray radiation has been described with the 3 foreseen cases of occurrence. Their associated power loads and localisation have been presented. The implication of the cross-polarisation case has been presented for different diagnostic systems. While the systems should be able to sustain the load for limited time, more work is required to evaluate the effects of long time exposure and to design mitigation strategies.

*The views and opinions expressed herein do not necessarily reflect those of the ITER Organization.*

#### References

- [1] M. Henderson, *The targeted heating and current drive applications for the ITER electron cyclotron system*, *Phys. Plasmas* **22**, 021808 (2015)
- [2] E. Poli, *TORBEAM, a beam tracing code for electron-cyclotron waves in tokamak plasmas*, *Computer Physics Communications* **136**, 90-104 (2001)
- [3] E. Mazzucato, *Relativistic effects on microwave reflectometry*, *Phys. Fluids B* **4**, 3460 (1992)
- [4] H.P. Laqua, *Distribution of the ECRH stray radiation in fusion devices*, *28th EPS Conference on Contr. Fusion and Plasma Phys.* **25A**, P3.099 (2001)
- [5] J.W. Oosterbeek, *Loads due to Stray Microwave Radiation in ITER*, *Fusion Engineering and Design*, submitted (2014)
- [6] M. Smith, *Analysis of ITER upper port diagnostic first wall*, *Fusion Science and Technology*, submitted (2015)
- [7] R. Reichle, *Review of the ITER diagnostics suite for erosion, deposition, dust and tritium measurements*, *Journal of Nuclear Materials*, submitted (2015)
- [8] H.J Hartfuss, *Fusion Plasma Diagnostics with mm-Waves: An Introduction*, Wiley-VCH (2013)